Available online at www.sciencedirect.com
ScienceDirect
Trans. Nonferrous Met. Soc. China 33(2023) 632−641
Transactions of Nonferrous Metals Society of China
www.tnmsc.cn

Effect of electric field on leaching valuable metals from spent lithium-ion batteries

Jian YANG[1,2,3], Yuan ZHOU[3], Zong-liang ZHANG[3],
Kai-hua XU[1,2], Kun ZHANG[1,2], Yan-qing LAI[3], Liang-xing JIANG[3]

1. Postdoctoral Research Station of GEM Co., Ltd., Shenzhen 518000, China;
2. Jingmen GEM New Material Co., Jingmen 448000, China;
3. School of Metallurgy and Environment, Central South University, Changsha 410083, China

Received 24 September 2021; accepted 22 March 2022

Abstract: An electric field enhanced leaching process was proposed to improve the leaching efficiency in the process of extracting Li, Ni, Co and Mn from waste lithium ion batteries. The leaching process was optimized and the leaching mechanism was studied by means of leaching experiments, product characterization and leaching kinetics. Under the optimized leaching conditions, more than 98% Li, 97% Ni and Co and 93% Mn were leached into the solution. The study of leaching kinetics shows that the leaching process of Li, Ni, Co and Mn is controlled by chemical reaction based on nuclear reduction model, and the activation energy of leaching is determined to be 42.4, 46.1, 46.2 and 47.3 kJ/mol, respectively. During the leaching process, the application of electric field provides a convenient channel for the recycling of Fe^{2+} and Cl^- in the solution, reduces the amount of reducing agent added, and ensures high metal leaching rate.

Key words: spent lithium-ion batteries; valuable metals leaching; electric field enhancement; leaching kinetics

1 Introduction

With rapid development of new electric vehicle, the installed capacity of lithium-ion battery (LIB, $LiMnO_4$, $LiCoO_2$, $LiNi_xCo_yMn_{1-x-y}O_2$, and $LiFePO_4$) has greatly increased usage [1]. Consequently, there has been dramatic increase in the number of spent LIBs due to their limited life span. LIBs contain metals (5−20% Co, 5−10% Ni, and 5% Li), electrolyte (15%), and plastic (7%), with compositions varying between manufacturers and end user [2−4]. Inappropriate spent LIB management poses significant biological and environmental health risk, whereas spent LIBs comprise a valuable waste resource, with potential for significant economic benefit by recovering the major components.

There are many recycling methods for valuable metals from spent LIBs, which can be broadly categorized as pyrometallurgical and hydrometallurgical processes [5,6]. Typical pyrometallurgical approaches involve crushing, roasting, oxide reduction, and refining and separating metals [7]. However, these processes have many shortcomings, including high energy consumption, low metal recovery rate, and particular difficulty to recover lithium [8]. In contrast, hydrometallurgical processes achieve higher metal recovery rates and lower energy consumption, and hence have become popular spent LIBs recycling technologies, where leaching is a key step [9]. Inorganic acid leaching [10−14], organic acid leaching (e.g. citric, oxalic, lactic acids, etc. [15,16]), ammonia leaching [17], and bioleaching [18] are key technologies to extract the

Corresponding author: Liang-xing JIANG, Tel: +86-15116335788, E-mail: lxjiang@csu.edu.cn
DOI: 10.1016/S1003-6326(22)66134-X

valuable metals from spent LIBs. However, only sulfuric acid leaching has been industrialized, and more efficient reducing agents are required to enhance metal leaching [19]. H_2O_2 is the most common reducing agent, but suffers from poor stability, high price and difficult long-term storage [20]. No reducing agent is required when leaching with HCl [21] due to Cl^- reducibility, but HCl is volatile and corrosive.

Various chloride components have been proposed as reducing agents, e.g. NaCl and NH_4Cl, for non-hydrochloric acid systems to avoid these problems. For example, DUTTA et al [22] used ammonium chloride as the reducing agent in a sulfuric acid system to extract Li, Ni, Co and Mn from spent LIBs, achieving leaching rates more than 97% for these metals under 2.5 mol/L H_2SO_4 and 0.8 mol/L NH_4Cl conditions. However, leaching must be performed in a high acid system to ensure high metal leaching rates and throughput, which greatly increases workloads for subsequent treatments.

Electric field enhanced leaching offers high leaching efficiency, inexpensive operation and environmental friendliness. Hence, various such systems have been employed to extract metals from solid materials [23], including vanadium leaching from converter slag [24], manganese leaching from furnace dust [25], copper leaching [26], gold leaching, and heavy metal-polluted soil remediation [27].

However, no previous study has reported enhanced Li, Ni, Co, and Mn extraction from spent LIBs using electric fields. Therefore, in this work, applied electric field effects on leaching processes considering processing conditions, and leaching kinetics and mechanisms were investigated, providing reference points to efficiently extract valuable metals from spent LIBs.

2 Experimental

2.1 Pretreatment for spent LIBs

The spent LIBs used in the experiments were supplied by Hunan Ye Xiang Technology Co., Ltd. (Changsha, China). First, the spent LIBs were discharged in 5% NaCl solution to avoid self-ignition and explosion caused by battery residual voltage. Second, the cathode electrodes of spent LIBs were collected by manual disassembly and cutting of the cathode electrodes into small pieces of about 2 cm × 2 cm. Then, the cut pieces were placed in a muffle furnace and kept at 400 °C for 2 h. The samples were cooled down to room temperature and the active substance powders were removed from the aluminum foil current collector.

2.2 Leaching of active substance powders

Figure 1 shows the enhanced leaching experiment equipment, including a beaker immersed in a constant temperature water bath with magnetic stirring. Both anode and cathode electrodes for all leaching experiments were graphite and powered by a DC power supply. The electrodes were welded with a plastic isolated copper wire, and sealed with epoxy resin, leaving only 16 cm^2 (4 cm × 4 cm) as the working area. The required cathode active material dosage, NaCl, and $FeSO_4$ were estimated and added to a designated volume of dilute H_2SO_4 solution at a fixed temperature. The power supply was then turned on and the current was adjusted to the desired level. Agitation was set to 600 r/min for all leaching experiments. The slurry was agitated with a magnetic stirrer for a specific time period, followed by filtration. Leaching rate (η_{Me}) for the target metals was calculated as

$$\eta_{Me}=\frac{C_{Me}\cdot V_{liquid}}{m\cdot w_{Me}}\times 100\% \quad (1)$$

where C_{Me} is the concentration of metal ions in the leachate, V_{liqiud} is the volume of leachate, m represents the mass of the cathode powder, and w_{Me} represents the mass fraction of metal in cathode powder.

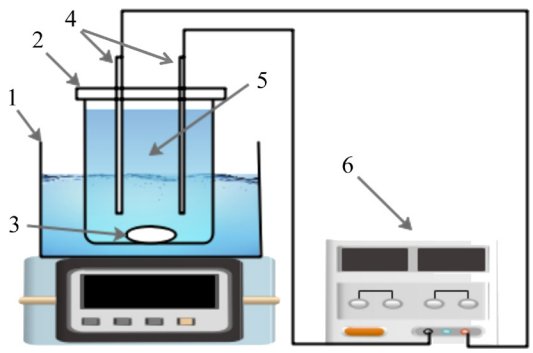

Fig. 1 Leaching experiment setup: 1−Magnetic stirring water bath; 2−Closed electrolytic cell; 3−Magnetic rotor; 4−Electrodes; 5−Pulp; 6−Constant current power supply

2.3 Characterization

Concentrations for Li^+, Ni^{2+}, Co^{2+} and Mn^{2+} in leachate were measured by ICP-OES (iCAP 7400, China), with mean composition of 29.6%, 7.03%, 16.7% and 11.5% for Ni, Li, Mn and Co, respectively, with other metals (Cu, Al and Fe) less than 0.2%. X-ray diffraction (XRD) patterns were measured using a Bruker X-ray diffraction with Cu K_α radiation at 30 mA and 30 kV, with 2θ of 5°−70°. Scanning electron microscope (SEM) images were obtained using an FEI-TESCAN microscope.

3 Results and discussion

3.1 Effect of parameters on leaching process

3.1.1 H_2SO_4 concentration

Figure 2 shows effects of H_2SO_4 concentration (0.5−3.0 mol/L) on metal leaching from spent LIBs at 80 °C, 80 g/L solid-to-liquid (S/L) ratio, 20 g/L NaCl, 200 A/m^2 current density, and 0.1 mol/L $FeSO_4$ for 60 min. All metal leaching rates increased with increasing H_2SO_4 concentration. Chemical valences for Co and Mn in ternary NCM materials are +3 and +4, respectively. MnO_2 and Co_2O_3 exhibited stronger oxidation capacity in high acid systems, following their E−pH diagrams [28], which is beneficial to enhancing reduction by Fe^{2+} and Cl^-, and hence increased metal leaching rate. Increasing H_2SO_4 concentration could also increase collision frequency between leaching agent and cathode material powders, increasing the leaching rate [29]. Leaching rates for Li, Ni, Co and Mn reached 98.2%, 97.1%, 96.3% and 93.2%, respectively, for 2.0 mol/L H_2SO_4, then remained unchanged with further H_2SO_4 concentration increasing. Therefore, 2.0 mol/L sulfuric acid was suitable for leaching.

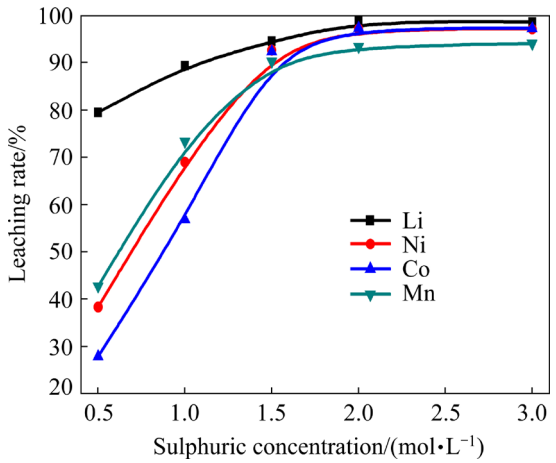

Fig. 2 Effects of H_2SO_4 concentration on metal leaching rate (80 g/L S/L ratio, 80 °C, 200 A/m^2 current density, 0.1 mol/L $FeSO_4$, and 20 g/L NaCl for 60 min)

3.1.2 Current density

Figure 3 shows metal leaching rate with respect to current density. Leaching valuable metals from active materials could work even without applying an electric field, due to Fe^{2+} and Cl^- reduction. However, leaching rate increased significantly by applying an electric field. That may be because newly formed Fe^{3+} was reduced to Fe^{2+} again on the cathode surface, which re-engages it in the leaching reaction and thus contributes to the increased metal leaching rate. Maximum metal leaching rates were achieved at 200 A/m^2. However, the leaching rate tends to fall away with further current density increase, which may be because Mn^{2+} in solution is oxidized to MnO_2 on the anode surface, and Ni^{2+} and Co^{2+} in solution are reduced to Ni and Co on the cathode surface at high current densities. Therefore, 200 A/m^2 of current density was suitable for leaching.

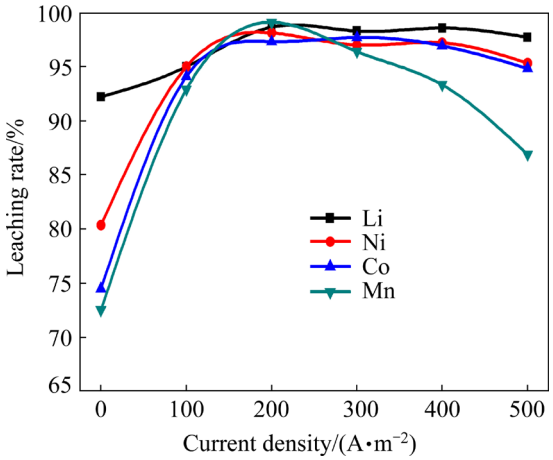

Fig. 3 Effects of current density on metal leaching rate (2.0 mol/L H_2SO_4, 80 °C, 80 g/L S/L ratio, 0.1 mol/L $FeSO_4$ and 20 g/L NaCl for 60 min)

3.1.3 Leaching temperature

Figure 4 shows that metal leaching rates increase with increasing leaching temperature. That may be attributed to reduced redox potential for Cl_2/Cl^- as temperature increased, which also increased overlapping voltage between Cl_2/Cl and MnO_2/Mn^{2+} as well as $Co(OH)_3/Co^{2+}$, and enhanced Co(III) and Mn(IV) reduction in solid oxide phase to Co(II) and Mn(II) [30]. Leaching reactions are endothermic, hence increased temperature increases leaching rate [5]. Average molecule kinetic energy

increases with increasing temperature, causing more frequent and energetic collisions between molecules, and hence increased the leaching reaction efficiency. Maximum metal leaching rates were 98.2%, 97.1%, 96.3% and 93.2% for Li, Ni, Co and Mn, at 80 °C respectively. However, metal leaching rates tended plateau for temperature above 80 °C, hence 80 °C was optimal for leaching.

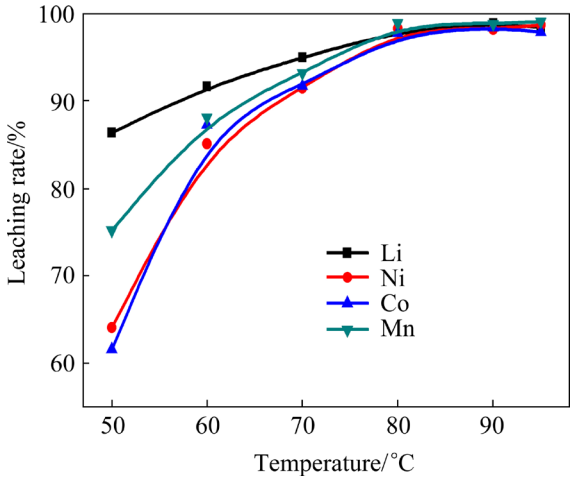

Fig. 4 Effects of temperature on metal leaching rate (2.0 mol/L H_2SO_4, 80 g/L S/L ratio, 200 A/m^2 current density, 0.1 mol/L $FeSO_4$, and 20 g/L NaCl for 60 min)

3.1.4 NaCl concentration

Figure 5 shows the metal leaching rates regarding NaCl concentration. The leaching rates of metal showed a gradual upward trend with the increase of NaCl concentration. That may be because increasing NaCl concentration increases the chloride ion concentration, which can react with cathode materials, promoting metal leaching from spent LIBs. In addition, Cl^- is discharged at the anode first, which can reduce the amount of Mn oxidized at the anode [16]. The leaching rates of metal reached the maximum when the NaCl concentration was 20 g/L. However, the leaching rate of Ni, Co and Mn tended to be unchanged when the NaCl concentration was higher than 20 g/L. Therefore, 20 g/L NaCl was suitable for the leaching process.

3.1.5 $FeSO_4$ concentration

The results of metal leaching rate from spent LIBs to the $FeSO_4$ concentration are shown in Fig. 6. Leaching rates for Ni, Co and Mn increased with even small increased $FeSO_4$ concentration due to Fe^{2+} reducibility. Fe^{2+} can promote the conversion of Cl_2 which is generated during leaching into Cl^- (Eq. (2)) and then reduce the chlorine spillover to realize the recycling of chlorine in solution. When an electric field is present, newly formed Fe^{3+} is discharged at the cathode in preference to H^+ and converted to Fe^{2+} on the cathode surface (Eq. (3)), which enables the recycling of Fe^{2+} and also helps to retain higher solution acidity [21]. Over 98% Li, 97% Ni, 96% Co, and 93% Mn can be leached when the $FeSO_4$ concentration was 0.1 mol/L. There is little change in the metal leaching rates with further increased $FeSO_4$ concentration. Therefore, 0.1 mol/L $FeSO_4$ was suitable for the leaching process.

$$Cl_2+2Fe^{2+}=2Cl^-+2Fe^{3+} \quad (2)$$

$$Fe^{3+}+e=Fe^{2+} \quad (3)$$

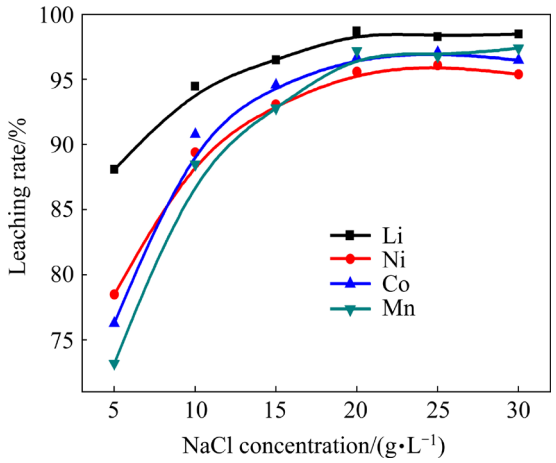

Fig. 5 Effects of NaCl concentration on leaching rate of metals (2.0 mol/L H_2SO_4, 80 °C, 200 A/m^2 current density, 0.1 mol/L $FeSO_4$ and 80 g/L S/L ratio for 60 min)

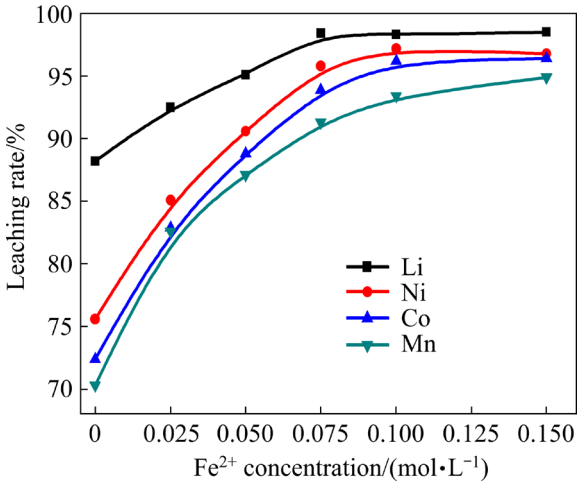

Fig. 6 Effects of Fe^{2+} concentration on leaching rate of metals (2.0 mol/L H_2SO_4, 80 °C, 200 A/m^2 current density, 80 g/L S/L ratio, and 20 g/L NaCl for 60 min)

3.1.6 Solid-to-liquid ratio

Figure 7 shows that metal leaching rates for all considered metals remained relatively constant for S/L ratio <80 g/L, and reduced with increasing S/L ratio (>80 g/L). Increased S/L ratio reduces the effective surface area for each particle in the unit volume to take part in the reaction and hence weakens metal leaching; whereas lower S/L ratio helps acid molecule diffusion from the solid/liquid interface to the bulk solution, promoting the leaching [17]. Thus, almost all metals could be leached out for S/L ratio of 80 g/L which was selected as the optimum condition.

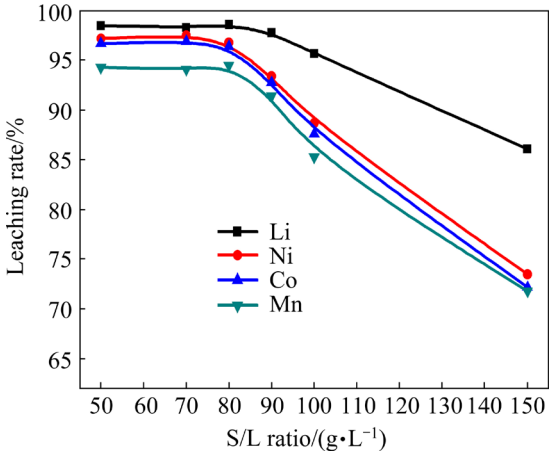

Fig. 7 Effects of solid−liquid ratio on leaching rate of metals (2.0 mol/L H_2SO_4, 80 °C, 200 A/m^2 current density, 0.1 mol/L $FeSO_4$, and 20 g/L NaCl for 60 min)

3.2 Apparent kinetics of leaching

Figure 8 shows timelines for metal leaching rates at different leaching temperatures. Metal leaching rates gradually increase with prolonged leaching time, with shorter leaching time required to reach maximum leaching rate at higher temperatures. Maximum leaching rate was achieved for all metals after leaching for 60 min at 80 °C.

The leaching process includes reactive ion diffusion within the liquid film surface, then the subsequent diffusion into the inner core surface, and reactions on the inner core surface. Following the previous studies [31,32], the chemical reaction

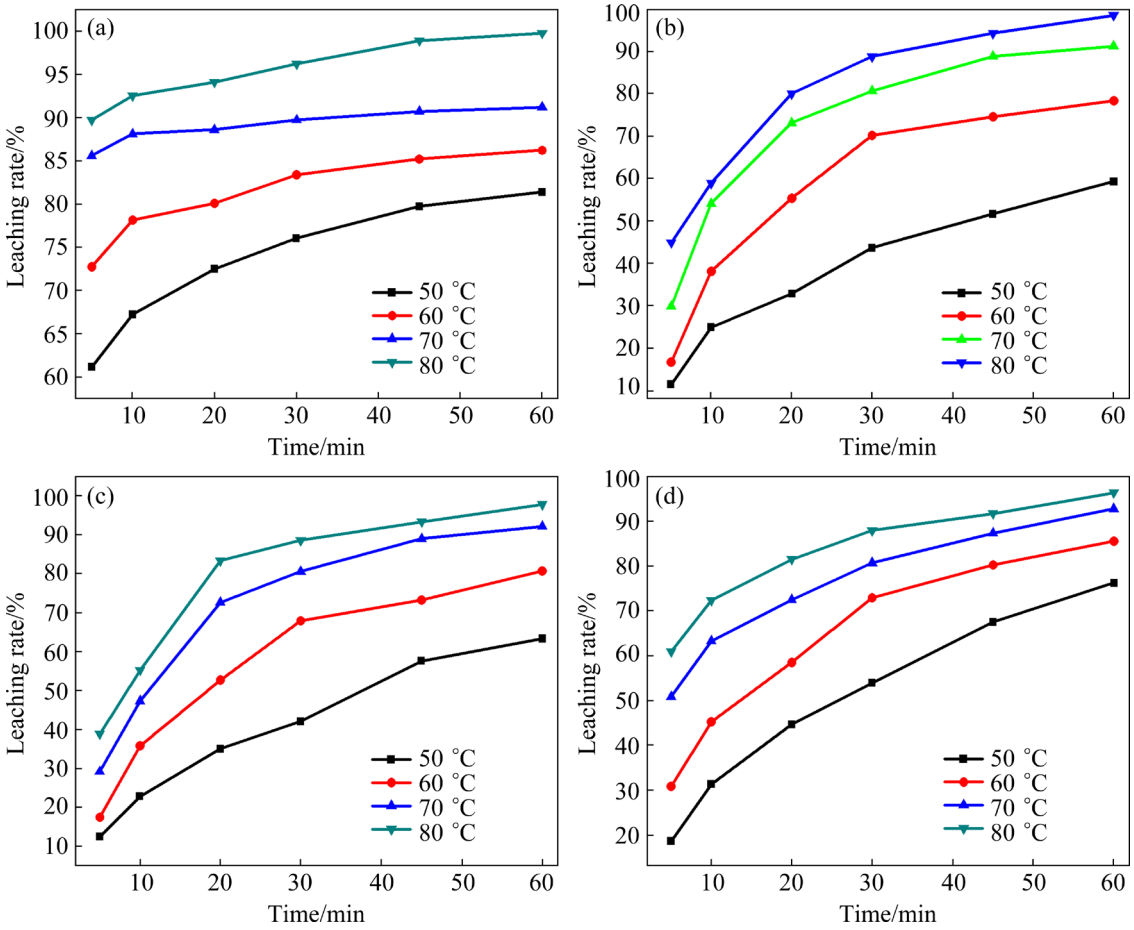

Fig. 8 Effect of temperature on leaching rate of metals at different time intervals: (a) Li; (b) Ni; (c) Co; (d) Mn (2.0 mol/L H_2SO_4, 80 g/L S/L ratio, 200 A/m^2 current density, 0.1 mol/L $FeSO_4$, and 20 g/L NaCl)

control model (Eq. (4)), diffusion control model (Eq. (5)), logarithmic rate law model (Eq. (6)), and Avrami equation model (Eq. (7)) were applied to analyzing the leaching mechanisms [33].

$$1-(1-x)^{1/3}=k_a t \tag{4}$$

$$1-\frac{2}{3}x-(1-x)^{2/3}=k_b t \tag{5}$$

$$[-\ln(1-x)]^2=k_c t \tag{6}$$

$$\ln[-\ln(1-x)]=\ln k_d+n\ln t \tag{7}$$

where x is the leaching rate of metal corresponding to leaching time t, and k_a, k_b, k_c and k_d represent the rate constant of chemical reactions.

As shown in Fig. 9, the data of the leaching process on kinetics fitted well to the Avrami equation model, which is evident from the high R^2 values (>0.98). The Arrhenius equation (Eq. (8)) can represent the relationship between specific rate constant and temperature, and hence the activation energy can be estimated. As shown in Fig. 10, the leaching activation energy of Li, Ni, Co and Mn during leaching was estimated as 42.4, 46.1, 46.2, and 47.3 kJ/mol, respectively. They are all over 40 kJ/mol, which is typical for chemical reaction controlled processes.

$$k=A\exp\frac{-E_a}{RT} \tag{8}$$

where k represents the rate constant of reaction, A and E_a represent the frequency factor and apparent activation energy, respectively, T is the thermodynamic temperature, and R represents the molar gas constant.

3.3 XRD patters of samples

The XRD patterns of the electrode powders used in the experiments before and after leaching are shown in Fig. 11. The original sample exhibits the characteristic $LiNi_{0.5}Co_{0.2}Mn_{0.3}O_2$ peak, with significantly weak peaks after leaching. That may be due to collapsing $LiNi_{0.5}Co_{0.2}Mn_{0.3}O_2$ layered structure by leaching agent erosion during leaching, reducing the residue phase crystallinity. Some

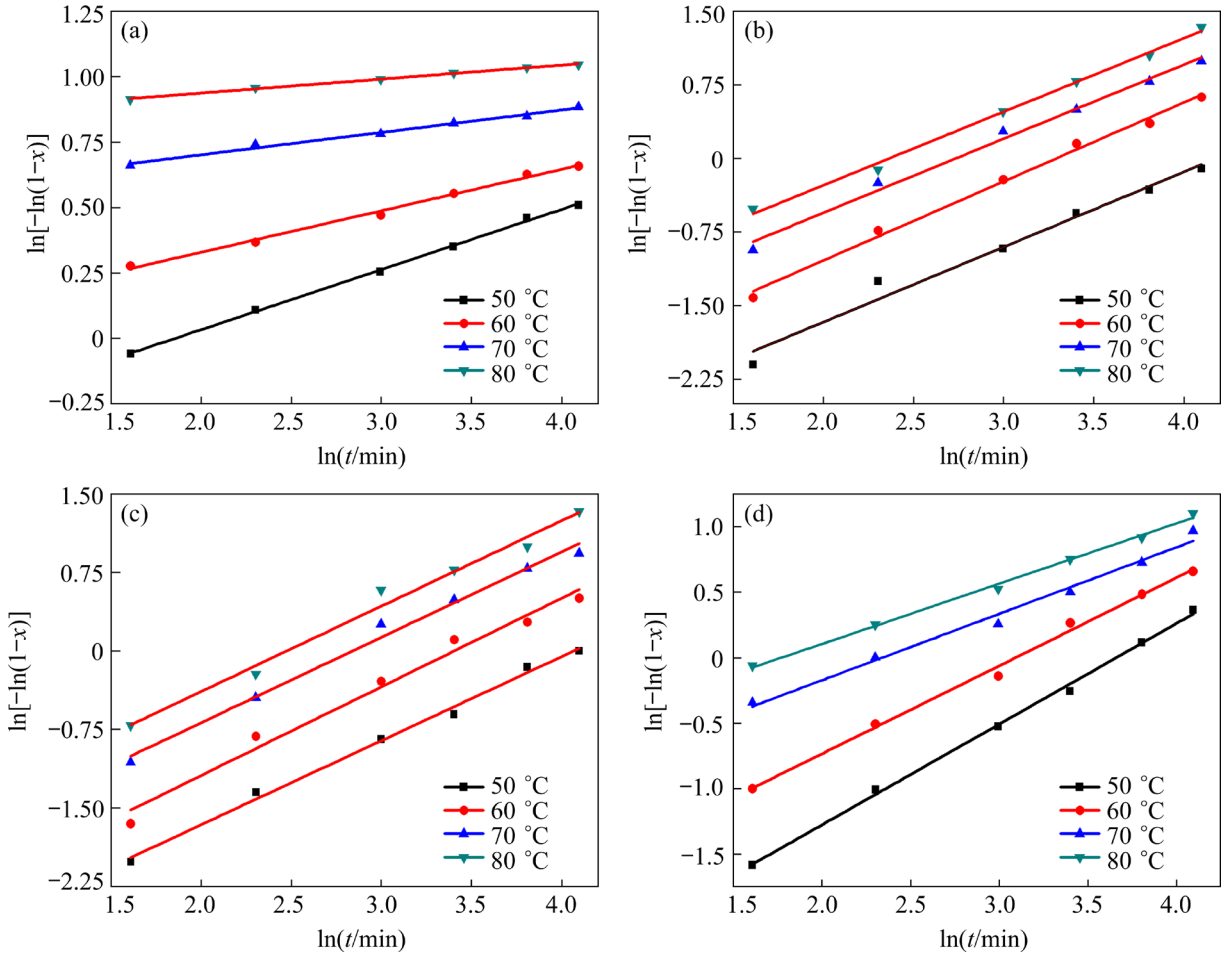

Fig. 9 Avrami equation model fitting parameters of metal elements during leaching process: (a) Li; (b) Ni; (c) Co; (d) Mn

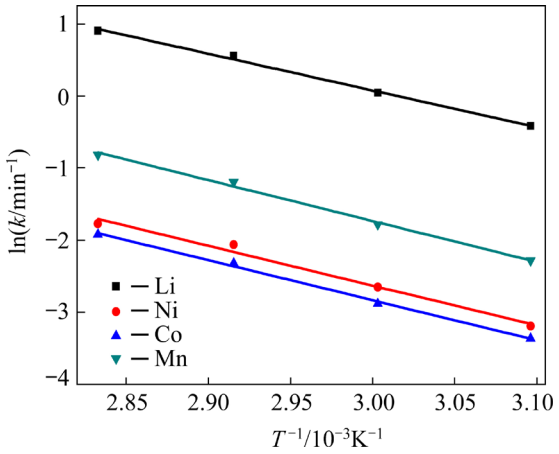

Fig. 10 Arrhenius fitting for Li, Ni, Co and Mn during leaching process

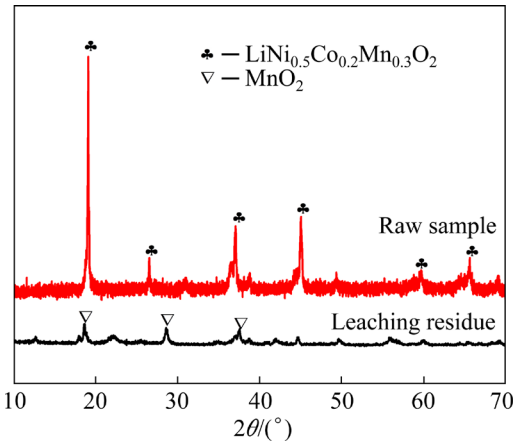

Fig. 11 XRD patterns of leaching residues and raw sample

heterogeneous peaks appear in the leached residue, which is the characteristic of MnO_2 and consistent with results from lower Mn leaching rate during leaching.

To clarify the microscopic morphological changes in the samples before and after leaching, SEM tests were carried out and the results are shown in Fig. 12. It can be seen that the microscopic morphology of the sample changes before and after leaching. Before leaching, the sample comprised well-defined spherical particles that can be resolved in accumulation of much finer primary particles at higher magnification. However, the sample comprises amorphous particles with a loose structure after

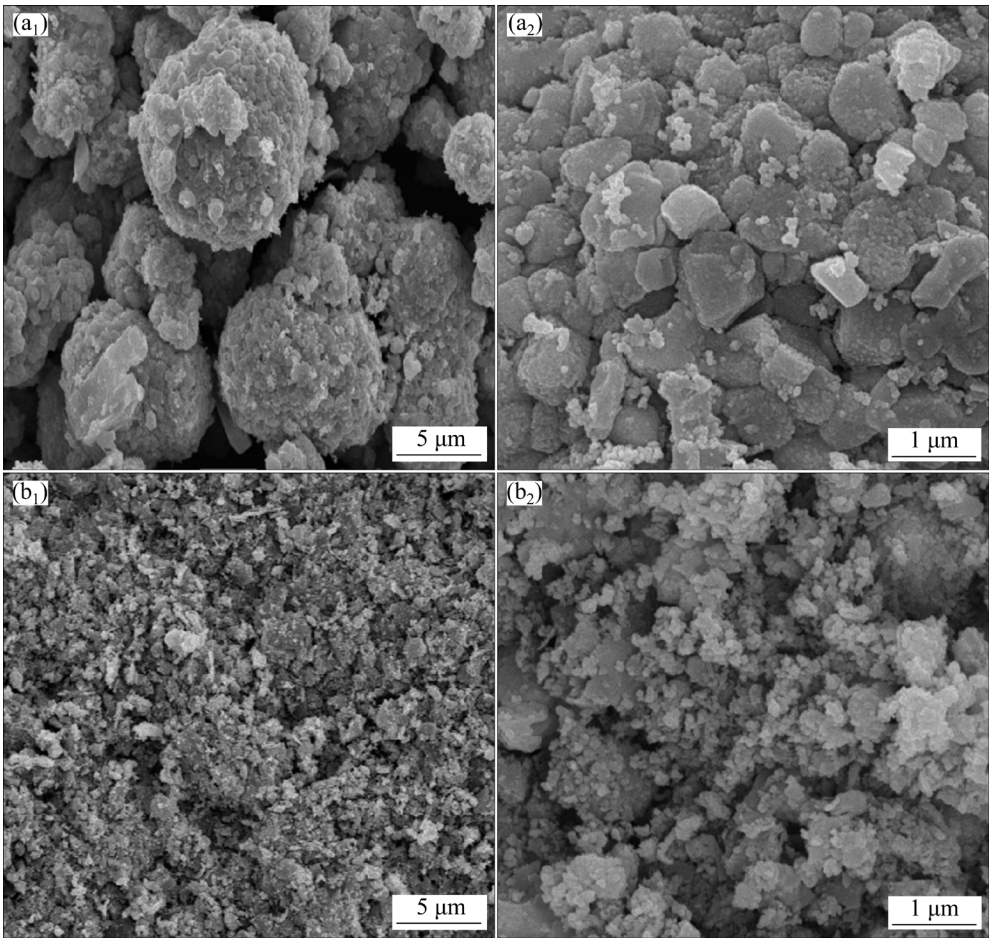

Fig. 12 SEM images of sample before (a_1, a_2) and after (b_1, b_2) leaching

leaching and these agglomerates do not change morphology at higher magnification. Combined with the results of the XRD pattern analysis of the leached residue, it can be deduced that the main composition for the loose amorphous particles is MnO_2. The poor crystallinity of the amorphous particles leads to a weakening of the characteristic peaks in the corresponding XRD pattern, which is consistent with the XRD pattern of the residue phase.

3.4 Leaching mechanism

Normally, Cl^- acts as a reducing agent during leaching and reacts with $LiNi_{0.5}Co_{0.2}Mn_{0.3}O_2$. However, leaching reactions produce enormous Cl_2 that overflows from the solution. Introducing Fe^{2+} can reduce Cl_2 overflow based on the redox reaction and maintain Cl^- concentration in solution at a high level. Applying an external electric field reduces formed Fe^{3+} to Fe^{2+} on the cathode surface, realizing Fe^{2+} reuse. Therefore, the H_2SO_4+NaCl+$FeSO_4$ synergistic leaching system can realize Cl^- and Fe^{2+} recycling by introducing an electric field, reducing agent dosage while maintaining high metal leaching rates. Water electrolysis reactions also occur in the system on the cathode and anode, respectively. Figure 13 shows reaction processes during leaching.

$$2H^+ + 2e \rightarrow H_2 \quad (\varphi^\Theta = 0\ \text{V, cathode}) \tag{9}$$

$$H_2O \rightarrow 2H^+ + 1/2O_2 + 2e \quad (\varphi^\Theta = 1.229\ \text{V, anode}) \tag{10}$$

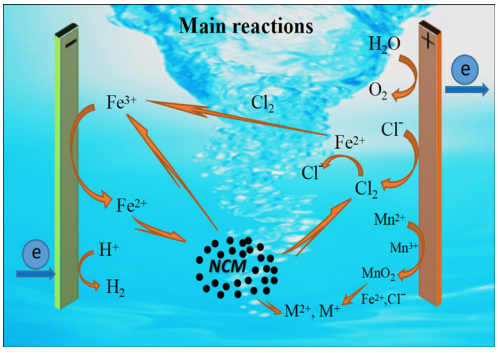

Fig. 13 Mechanism for electric field enhanced metal leaching process

The synergistic effect of Fe^{2+}, Cl^-, and electric field on the metal leaching rates was verified by comparative experiments, and the results are shown in Fig. 14. Compared with other comparison experiments, the metal leaching rates increased when Fe^{2+} and Cl^- were simultaneously present in the solution and an external electric field was applied. Chloride concentration in H_2SO_4 + NaCl + $FeSO_4$ leaching solution did not change greatly before and after leaching when the electric field was applied (Table 1), improving effective Cl^- utilization and reducing Cl_2 overflow leachate obtained after leaching could be used for Ni−Co alloy and MnO_2 electrodeposition, which is the focus for ongoing research.

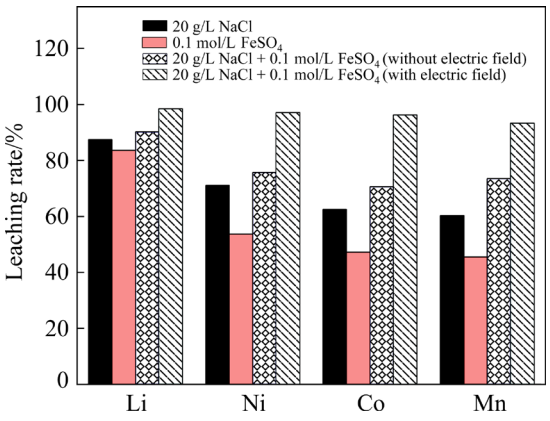

Fig. 14 Metal leaching rates under different leaching conditions (2.0 mol/L H_2SO_4, 80 g/L S/L ratio, 80 °C, 60 min, and 200 A/m^2 current density)

Table 1 Concentration of Cl^- in solution with and without electric field applied (g/L)

Leaching system	Before leaching	After leaching
Without electric field	12.1	3.1
With electric field	12.1	11.4

4 Conclusions

(1) Metal leaching rates increased in the presence of an electric field when Fe^{2+} and Cl^- were simultaneously present in the solution compared to leaching without an electric field.

(2) Generated Cl_2 during leaching can be reduced to Cl^- by Fe^{2+} by adopting Fe^{2+} and Cl^- synergistic leaching, reducing formed Fe^{3+} to Fe^{2+} on the surface of the cathode, and hence enabling Fe^{2+} and Cl^- recycling.

(3) More than 98%, 97%, 96% and 93% extraction for Li, Ni, Co and Mn, respectively, could be leached under 2.0 mol/L H_2SO_4, 20 g/L NaCl, 0.1 mol/L $FeSO_4$, S/L ratio 80 g/L, current density 200 A/m^2, leaching temperature 80 °C, and leaching time >60 min.

(4) Leaching kinetics confirmed that leaching was governed by chemical reaction control based on the nuclear reduction model, with apparent activation energies of 42.4, 46.1, 46.2, and 47.3 kJ/mol for Li, Ni, Co and Mn, respectively, during leaching.

Acknowledgments

This work was supported by the National Natural Science Foundation of China (No. 51674298), and Anhui Province Research and Development Innovation Program, China.

References

[1] WU Fang. Recovery of cobalt and lithium from spent lithium-ion secondary batteries [J]. The Chinese Journal of Nonferrous Metals, 2004, 14(4): 697−701. (in Chinese)

[2] REN Guo-xing, XIAO Song-wen, XIE Mei-qiu, PAN Bing, CHEN Jian, WANG Feng-gang, XIA Xing. Recovery of valuable metals from spent lithium ion batteries by smelting reduction process based on $FeO-SiO_2-Al_2O_3$ slag system [J]. Transactions of Nonferrous Metals Society of China, 2017, 27(2): 450−456.

[3] LI Jin-long, HE Ya-qun, FU Yuan-peng, XIE Wei-ning, FENG Yi, ALEJANDRO K. Hydrometallurgical enhanced liberation and recovery of anode material from spent lithium-ion batteries [J]. Waste Management, 2021, 126(5): 517−526.

[4] ZHU Shu-guang, HE Wen-zhi, LI Guang-ming, ZHOU Xu, ZHANG Xiao-jun, HUANG Ju-wen. Recovery of Co and Li from spent lithium-ion batteries by combination method of acid leaching and chemical precipitation [J]. Transactions of Nonferrous Metals Society of China, 2012, 22(9): 2274−2281.

[5] YANG Jian, JIANG Liang-xing, LIU Fang-yang, JIA Ming, LAI Yan-qing. Reductive acid leaching of valuable metals from spent lithium-ion batteries using hydrazine sulfate as reductant [J]. Transactions of Nonferrous Metals Society of China. 2020, 30(8): 2256−2264.

[6] KIM S, BANG J, YOO J, SHIN Y, BAE J, JEONG J, KIM K, DONG Peng, KWON K. A comprehensive review on the pretreatment process in lithium-ion battery recycling [J]. Journal of Cleaner Production, 2021, 294(524): 126329.

[7] CHU Wei, ZHANG Ya-li, CHEN Lin-lin, WU Kai-peng, HUANG Yao-guo, JIA Yun. Comprehensive recycling of Al foil and active materials from the spent lithium-ion battery [J]. Separation and Purification Technology, 2021, 269: 118704.

[8] LIU Wei-feng, FU Xin-xin, YANG Tian-zu, ZHANG Du-chao, CHEN Lin. Oxidation leaching of copper smelting dust by controlling potential [J]. Transactions of Nonferrous Metals Society of China, 2018, 28(9): 1854−1861.

[9] EBRAHIMZADE H, KHAYATI G R, SCHAFFIE M. Thermal decomposition kinetics of basic carbonate cobalt nanosheets obtained from spent Li-ion batteries: Deconvolution of overlapping complex reactions [J]. Transactions of Nonferrous Metals Society of China, 2018, 28(6): 1265−1274.

[10] LIU Chun-wei, LIN Jiao, CAO Hong-bin, ZHANG Yi, SUN Zhi. Recycling of spent lithium-ion batteries in view of lithium recovery: A critical review [J]. Journal of Cleaner Production, 2019, 228: 801−813.

[11] HE Feng, MAN Rui-lin, LIU Qi, SUN Zu-mei, XU Jian, ZHANG Jian. Kinetics of acid leaching cobalt from waste lithium-ion batteries using oat straw [J]. The Chinese Journal of Nonferrous Metals, 2015, 25(4): 1103−1108. (in Chinese)

[12] LI Hao-yu, YE Hua, SUN Ming-cang, CHEN Wu-jie. Process for recycle of spent lithium iron phosphate battery via a selective leaching-precipitation method [J]. Journal of Central South University, 2020, 27(11): 3239−3248.

[13] YANG Jian, QIN Ji-tao, LI Fang-cheng, JIANG Liang-xing, LAI Yan-qing, LIU Fang-yang, JIA Ming. Review of hydrometallurgical processes for recycling spent lithium-ion batteries [J]. Journal of Central South University (Science and Technology), 2020, 51(12): 3261−3278. (in Chinese)

[14] DENG Xiao-rong, ZENG Gui-sheng, LUO Sheng-lian, LUO Xu-biao, ZOU Jian-ping. Electrochemical behavior of bioleaching $LiCoO_2$ from spent lithium-ion batteries by *Thiobacillus ferrooxidans* [J]. Journal of Central South University (Science and Technology), 2012, 43(7): 2500−2505. (in Chinese)

[15] GOLMOHAMMADZADEH R, FARAJI F, RASHCHI F. Recovery of lithium and cobalt from spent lithium ion batteries (LIBs) using organic acids as leaching reagents: A review [J]. Resources, Conservation and Recycling, 2018, 136: 418−435.

[16] GUO Miao-miao, XI Xiao-li, ZHANG Yun-he, YU Shun-wen, LONG Xiao-lin, JIANG Zheng-kang, NIE Zuo-ren, XU Kai-hua. Recovering valuable metals from waste ternary cathode materials of power battery by combined high temperature hydrogen reduction and hydrometallurgy [J]. The Chinese Journal of Nonferrous Metals, 2020, 30(6): 1415−1426. (in Chinese)

[17] SETIAWAN H, PETRUS H T B M, PERDANA I. Reaction kinetics modeling for lithium and cobalt recovery from spent lithium-ion batteries using acetic acid [J]. International Journal of Minerals Metallurgy and Materials, 2019, 26(1): 98−107.

[18] LI Mi, PENG Bing, CHAI Li-yuan, PENG Ning, XIE Xian-de, YAN Huan. Technological mineralogy and environmental activity of zinc leaching residue from zinc hydrometallurgical process [J]. Transactions of Nonferrous Metals Society of China, 2013, 23(5): 1480−1488.

[19] MENG Qi, ZHANG Ying-jie, DONG Peng. Use of glucose as reductant to recover Co from spent lithium ions batteries [J]. Waste Management, 2017, 64: 214−218.

[20] PINNA E G, RUIZ M C, OJEDA M W, RODRIGUEZ M H. Cathodes of spent Li-ion batteries: Dissolution with phosphoric acid and recovery of lithium and cobalt from leach liquors [J]. Hydrometallurgy, 2017, 167: 66−71.

[21] LV Wei-guang, WANG Zhong-hang, CAO Hong-bin, ZHENG Xiao-hong, JIN Wei, ZHANG Yi, SUN Zhi. A

sustainable process for metal recycling from spent lithium-ion batteries using ammonium chloride [J]. Waste Management, 2018, 79: 545−553.

[22] DUTTA D, KUMARI A, PANDA R, JHA S, GUPTA D, GOEL S, JHA M K. Close loop separation process for the recovery of Co, Cu, Mn, Fe and Li from spent lithium-ion batteries [J]. Separation and Purification Technology, 2018, 200: 327−334.

[23] XU You-qun, MAN Rui-lin, ZHANG Jian, LIU Qi, XU Jian, SUN Zu-mei. Electrolytic stripping-biomass acid leaching recycling spent Li-ion battery [J]. The Chinese Journal of Nonferrous Metals, 2014, 24(10): 2576−2581. (in Chinese)

[24] LI Li, BIAN Yi-nan, ZHANG Xiao-xiao, GUAN Yi-biao, FAN E, WU Feng. Process for recycling mixed-cathode materials from spent lithium-ion batteries and kinetics of leaching [J]. Waste Management, 2018, 71: 362−371.

[25] YANG Yue, XU Sheng-ming, HE Ying-he. Lithium recycling and cathode material regeneration from acid leach liquor of spent lithium-ion battery via facile co-extraction and co-precipitation processes [J]. Waste Management, 2017, 64: 219−227.

[26] LIAO Jian-lin, WANG Yuan, SHAO Dan, ZHAO Rui-rui, CHEN Hong-yu. Recycling and reusing of $LiNi_{0.5}Co_{0.2}Mn_{0.3}O_2$ scrap for lithium ion batteries and investigation of material performance for lithium ion batteries [J]. The Chinese Journal of Nonferrous Metals, 2020, 30(9): 2171−2177. (in Chinese)

[27] YANG Jian, ZHANG Zong-liang, ZHANG Gang, JIANG Liang-xing, LIU Fang-yang, JIA Ming, LAI Yan-qing. Process study of chloride roasting and water leaching for the extraction of valuable metals from spent lithium-ion batteries [J]. Hydrometallurgy, 2021, 203: 105638.

[28] LAI Yan-qing, YANG Jian, ZHANG Gang, TANG Yi-wei, JIANG Liang-xing, YANG Sheng-hai, LI Jie. Optimization and kinetics of leaching valuable metals from cathode materials of spent ternary lithium ion batteries with starch as reducing agent [J]. The Chinese Journal of Nonferrous Metals, 2019, 29(1): 153−160. (in Chinese)

[29] WANG Bin, LIN Xin-ye, TANG Yuan-yuan, WANG Qiang, LEUNG M K H, LU Xiao-ying. Recycling $LiCoO_2$ with methanesulfonic acid for regeneration of lithium-ion battery electrode materials [J]. Journal of Power Sources, 2019, 436: 226828.

[30] YU Min, ZHANG Ze-hui, XUE Feng, YANG Bin, GUO Guang-hui, QIU Jiang-hua A more simple and efficient process for recovery of cobalt and lithium from spent lithium-ion batteries with citric acid [J]. Separation and Purification Technology, 2019, 215: 398−402.

[31] MESHRAM P, PANER B D, MANKHAND T R. Hydrometallurgical processing of spent lithium ion batteries (LIBs) in the presence of a reducing agent with emphasis on kinetics of leaching [J]. Chemical Engineering Journal, 2015, 281: 418−427.

[32] LI Li, BIAN Yi-Nan, ZHANG Xiao-xiao, XUE Qing, FAN ERSHA, WU Feng, CHEN Ren-jie. Economical recycling process for spent lithium-ion batteries and macro- and micro-scale mechanistic study [J]. Journal of Power Sources, 2018, 377: 70−79.

[33] LIU Peng-cheng, XIAO Li, CHEN Yi-feng, TANG Yi-wei, WU Jian, CHEN Han. Recovering valuable metals from $LiNi_xCo_yMn_{1-x-y}O_2$ cathode materials of spent lithium ion batteries via a combination of reduction roasting and stepwise leaching [J]. Journal of Alloys and Compounds, 2019, 783: 743−752.

电场对废旧锂离子电池中有价金属浸出的影响

杨 健[1,2,3]，周 媛[3]，张宗良[3]，许开华[1,2]，张 坤[1,2]，赖延清[3]，蒋良兴[3]

1. 深圳格林美股份有限公司 博士后科研工作站，深圳 518000；
2. 荆门市格林美新材料有限公司，荆门 448000；
3. 中南大学 冶金与环境学院，长沙 410083

摘 要：提出一种电场强化浸出工艺，用于提高废旧锂离子电池提取 Li、Ni、Co 以及 Mn 过程中的浸出效率。通过产品表征和浸出动力学等手段，对浸出工艺参数进行优化并对浸出机制进行研究。在优化浸出条件下，超过 98% Li、97% Ni 和 Co 以及 93% Mn 被浸出进入到溶液中。浸出动力学研究表明，Li、Ni、Co 和 Mn 的浸出过程由基于核缩减模型的化学反应控制，并确定浸出活化能分别为 42.4、46.1、46.2 和 47.3 kJ/mol。浸出过程中，施加电场为溶液中 Fe^{2+}和 Cl^-的循环利用提供了便利通道，减少了还原剂的添加量，同时保证了高的金属浸出率。

关键词：废旧锂离子电池；有价金属浸出；电场强化；浸出动力学

(Edited by Xiang-qun LI)